

# Thermal Conductivity and Large Isotope Effect in GaN from First Principles

L. Lindsay,<sup>1</sup> D. A. Broido,<sup>2</sup> and T. L. Reinecke<sup>1</sup>

<sup>1</sup>Naval Research Laboratory, Washington, D.C. 20375, USA

<sup>2</sup>Department of Physics, Boston College, Chestnut Hill, Massachusetts 02467, USA

(Received 15 June 2012; published 28 August 2012)

We present atomistic first principles results for the lattice thermal conductivity of GaN and compare them to those for GaP, GaAs, and GaSb. In GaN we find a large increase to the thermal conductivity with isotopic enrichment,  $\sim 65\%$  at room temperature. We show that both the high thermal conductivity and its enhancement with isotopic enrichment in GaN arise from the weak coupling of heat-carrying acoustic phonons with optic phonons. This weak scattering results from stiff atomic bonds and the large Ga to N mass ratio, which give phonons high frequencies and also a pronounced energy gap between acoustic and optic phonons compared to other materials. Rigorous understanding of these features in GaN gives important insights into the interplay between intrinsic phonon-phonon scattering and isotopic scattering in a range of materials.

DOI: [10.1103/PhysRevLett.109.095901](https://doi.org/10.1103/PhysRevLett.109.095901)

PACS numbers: 66.70.-f, 63.20.kg, 71.15.-m

**Introduction.**—Gallium nitride (GaN) is a wide band gap semiconductor and a promising candidate for use in optoelectronic devices [1,2], high-frequency switches [3,4], and high-power electronics [5]. Thermal management is of critical importance in such devices, especially as typical device sizes continue to decrease. GaN has the attractive feature of an unusually high lattice thermal conductivity,  $\kappa_L$ , with measured room temperature values around  $230 \text{ W m}^{-1} \text{ K}^{-1}$  [6–8]. To date, the origin of its high  $\kappa_L$  is not well understood at a quantitative level. Furthermore, increase of its  $\kappa_L$  could lead to better performing and longer-lived electronic devices.

As in other semiconductors, heat in GaN is carried primarily by phonons. The  $\kappa_L$  is limited by intrinsic phonon-phonon scattering around room temperature and higher [9] and by extrinsic scattering due to point defects such as isotopes. Recent work has estimated that the room temperature “isotope effect” given by  $P = 100 \times (\kappa_{\text{pure}}/\kappa_{\text{natural}} - 1)$  is a relatively small 4%–15% in GaN [6,10–12]. Here  $\kappa_{\text{pure}}$  corresponds to  $\kappa_L$  for isotopically pure GaN and  $\kappa_{\text{natural}}$  to  $\kappa_L$  with naturally occurring Ga isotope concentrations. Other work has suggested that  $\kappa_L$  of defect-free GaN is much larger than measured values but that the enhancement comes from removal of vacancies and substitutional defects rather than from isotope enrichment [13,14].

Reliable determination of  $\kappa_L$  and the effects of different scattering mechanisms depends on an accurate representation of the anharmonic phonon-phonon scattering. In simple models for  $\kappa_L$ , this scattering is often estimated by using a mode averaged Gruneisen constant and using parameters adjusted to fit measured data [10,11]. Such models lack predictive capability. Alternatively, molecular dynamics simulations have been used [15], but these cannot represent quantum mechanical scattering and so are of uncertain validity below the Debye temperature of a material ( $\sim 600 \text{ K}$  for GaN). In this Letter, we employ a first

principles approach to definitively determine  $\kappa_L$  in GaN due to phonon-phonon and isotopic impurity scattering. Unlike previous estimates, our state-of-the-art calculations show that the isotope effect in GaN is very large,  $\sim 65\%$  at room temperature, making it comparable to the highest isotope effects observed in diamond ( $\sim 50\%$ ) [16], graphene (60%) [17], and boron nitride nanotubes ( $\sim 50\%$ ) [18]. As a result, we find that the intrinsic upper limit to  $\kappa_L$  in GaN is around  $400 \text{ W m}^{-1} \text{ K}^{-1}$  at 300 K, considerably higher than currently measured  $\kappa_L$  values. We find that these features are a consequence of (i) the substantial isotope mixture in Ga, (ii) the large energy gap between the acoustic and optic phonons, and (iii) the high frequency scale of the phonon dispersion in GaN. The latter two points weaken the phonon-phonon scattering and, in particular, the scattering between the heat-carrying acoustic phonons and optic phonons. This leads to higher  $\kappa_L$  and makes isotope scattering relatively more important. We illustrate this effect by comparing the  $\kappa_L$  for GaN with that for GaAs, GaP, and GaSb.

**Ab initio thermal transport.**—We employ a first principles approach to calculate  $\kappa_L$ , which combines an exact numerical solution of the Peierls-Boltzmann transport equation with accurate calculations of the harmonic and anharmonic interatomic force constants (IFCs) using density functional theory and density functional perturbation theory. The absence of accurate values for the anharmonic IFCs has limited quantitative results for  $\kappa_L$  and full understanding of the underlying physics. A similar approach previously used by us has accurately described thermal transport in silicon, germanium, and diamond [19,20]. We consider  $\kappa_L$  limited by intrinsic (three-phonon) and isotope defect scattering processes. The thermal conductivity tensor is

$$\kappa_{\alpha\beta} = \frac{1}{(2\pi)^3} \sum_j \int (\partial n_{\lambda}^0 / \partial T) \hbar \omega_{\lambda} \nu_{\lambda\alpha} \nu_{\lambda\beta} \tau_{\lambda\beta} d\vec{q}. \quad (1)$$

Report Documentation Page				Form Approved OMB No. 0704-0188	
Public reporting burden for the collection of information is estimated to average 1 hour per response, including the time for reviewing instructions, searching existing data sources, gathering and maintaining the data needed, and completing and reviewing the collection of information. Send comments regarding this burden estimate or any other aspect of this collection of information, including suggestions for reducing this burden, to Washington Headquarters Services, Directorate for Information Operations and Reports, 1215 Jefferson Davis Highway, Suite 1204, Arlington VA 22202-4302. Respondents should be aware that notwithstanding any other provision of law, no person shall be subject to a penalty for failing to comply with a collection of information if it does not display a currently valid OMB control number.					
1. REPORT DATE <b>28 AUG 2012</b>		2. REPORT TYPE		3. DATES COVERED <b>00-00-2012 to 00-00-2012</b>	
4. TITLE AND SUBTITLE <b>Thermal Conductivity and Large Isotope Effect in GaN from First Principles</b>				5a. CONTRACT NUMBER	
				5b. GRANT NUMBER	
				5c. PROGRAM ELEMENT NUMBER	
6. AUTHOR(S)				5d. PROJECT NUMBER	
				5e. TASK NUMBER	
				5f. WORK UNIT NUMBER	
7. PERFORMING ORGANIZATION NAME(S) AND ADDRESS(ES) <b>Naval Research Laboratory, 4555 Overlook Ave SW, Washington, DC, 20375</b>				8. PERFORMING ORGANIZATION REPORT NUMBER	
9. SPONSORING/MONITORING AGENCY NAME(S) AND ADDRESS(ES)				10. SPONSOR/MONITOR'S ACRONYM(S)	
				11. SPONSOR/MONITOR'S REPORT NUMBER(S)	
12. DISTRIBUTION/AVAILABILITY STATEMENT <b>Approved for public release; distribution unlimited</b>					
13. SUPPLEMENTARY NOTES					
14. ABSTRACT					
15. SUBJECT TERMS					
16. SECURITY CLASSIFICATION OF:			17. LIMITATION OF ABSTRACT <b>Same as Report (SAR)</b>	18. NUMBER OF PAGES <b>5</b>	19a. NAME OF RESPONSIBLE PERSON
a. REPORT <b>unclassified</b>	b. ABSTRACT <b>unclassified</b>	c. THIS PAGE <b>unclassified</b>			

In Eq. (1),  $\omega_\lambda$  and  $\nu_{\lambda\alpha} = d\omega_\lambda/dq_\alpha$  are the frequency and  $\alpha$ th component of the velocity for a phonon in mode  $\lambda = (\vec{q}, j)$ , respectively, with wave vector  $\vec{q}$  in branch  $j$ ,  $n_\lambda^0$  is the Bose distribution function, and  $\tau_{\lambda\alpha}$  is the phonon lifetime. GaN has a wurtzite structure with an underlying hexagonal lattice. We define the layers to be in the  $x$ - $y$  plane with the  $c$  axis in the  $z$  direction. Then  $\kappa_{\alpha\beta}$  is diagonal with one out-of-plane component,  $\kappa_{zz}$ , and two in-plane components,  $\kappa_{xx}$  and  $\kappa_{yy}$ . In principle, for infinite, perfect hexagonal systems  $\kappa_{xx} = \kappa_{yy}$ , however,

isotope scattering introduces in-plane anisotropy. At around room temperature and higher, this anisotropy is only a few percent, so we define  $\kappa_{\text{in}} = (\kappa_{xx} + \kappa_{yy})/2$  and  $\kappa_{\text{out}} = \kappa_{zz}$  to discuss in-plane and out-of-plane thermal transport.

The linearized Peierls-Boltzmann transport equation is solved by using an iterative scheme described in detail previously [19–21]. The intrinsic three-phonon scattering probabilities are

$$\Gamma_{\lambda\lambda'\lambda''}^{(\pm)} = \frac{\hbar\pi}{4N_0\omega_\lambda\omega_{\lambda'}\omega_{\lambda''}} \left\{ \frac{n_{\lambda'}^0 - n_{\lambda''}^0}{n_{\lambda'}^0 + n_{\lambda''}^0 + 1} \right\} \left| \Phi_{\lambda,\pm\lambda',-\lambda''}^{(\pm)} \right|^2 \delta(\omega_\lambda \pm \omega_{\lambda'} - \omega_{\lambda''}), \quad (2)$$

$$\Phi_{\lambda\lambda'\lambda''} = \sum_{\kappa} \sum_{l'\kappa'} \sum_{l''\kappa''} \sum_{\alpha\beta\gamma} \Phi_{\alpha\beta\gamma}(0\kappa, l'\kappa', l''\kappa'') \frac{e_{\alpha\kappa}^\lambda e_{\beta\kappa'}^{\lambda'} e_{\gamma\kappa''}^{\lambda''}}{\sqrt{\bar{m}_\kappa \bar{m}_{\kappa'} \bar{m}_{\kappa''}}} e^{i\vec{q}' \cdot \vec{R}_{l'}} e^{i\vec{q}'' \cdot \vec{R}_{l''}}.$$

Here,  $N_0$  is the number of unit cells, and the  $\pm$  correspond to the three-phonon processes that satisfy conservation of energy and momentum:  $\omega_j(\vec{q}) \pm \omega_{j'}(\vec{q}') = \omega_{j''}(\vec{q}'')$  and  $\vec{q} \pm \vec{q}' = \vec{q}'' + \vec{K}$ , where  $\vec{K}$  is a reciprocal lattice vector, which is zero for normal processes and nonzero for umklapp processes [9]. Also,  $\Phi_{\alpha\beta\gamma}(0\kappa, l'\kappa', l''\kappa'')$  are third-order anharmonic IFCs,  $e_{\alpha\kappa}^\lambda$  is the  $\alpha$ th component of the phonon eigenvector  $\hat{e}_\kappa^\lambda$  for the  $\kappa$ th atom of the unit cell in mode  $\lambda$ , and  $\vec{R}_l$  is the lattice vector locating the  $l$ th unit cell. The scattering time due to isotopic impurities,  $\tau_\lambda^{\text{iso}}$ , is given by [22]

$$1/\tau_\lambda^{\text{iso}} = \frac{\pi}{2N_0} \omega_\lambda^2 \sum_{\kappa} g_\kappa \sum_{\lambda'} |\hat{e}_\kappa^\lambda \cdot \hat{e}_{\kappa'}^{\lambda'*}|^2 \delta(\omega_\lambda - \omega_{\lambda'}). \quad (3)$$

In Eq. (3),  $g_\kappa = \frac{1}{\bar{m}_\kappa} \sum_i f_{i\kappa} (m_{i\kappa} - \bar{m}_\kappa)^2$  is a mass variance parameter with  $f_{i\kappa}$  and  $m_{i\kappa}$  being the concentration and mass of the  $i$ th isotope of the  $\kappa$ th atom, respectively, and  $\bar{m}_\kappa$  being the average mass. For gallium (60.11%  $^{69}\text{Ga}$  and 39.89%  $^{71}\text{Ga}$ ),  $g_{\text{Ga}} = 1.97 \times 10^{-4}$ , while for N, the isotope variation is negligible,  $g_{\text{N}} = 0$ .

The formalism described above requires harmonic IFCs to calculate phonon frequencies and eigenvectors from diagonalization of the dynamical matrix. It also requires the  $\Phi_{\alpha\beta\gamma}(0\kappa, l'\kappa', l''\kappa'')$  to allow calculation of the matrix elements for phonon-phonon scattering in Eq. (2). These IFCs were calculated within the framework of density functional theory and density functional perturbation theory using norm-conserving pseudopotentials in the local density approximation (LDA) with the QUANTUM ESPRESSO package [23]. The ground state configuration for the wurtzite lattice was determined by varying the in-plane,  $a$ , and out-of-plane,  $c$ , lattice constants to find the minimum energy, and the internal parameter  $u$  was chosen so that the residual Hellman-Feynman forces on the atoms were zero. We find lattice constants that are 1.8% less than experiment ( $a_{\text{exp}} = 3.190 \text{ \AA}$ ,  $c_{\text{exp}} = 5.189 \text{ \AA}$ ,

and  $u_{\text{exp}} = 0.377$  [24]). This is consistent with a known shortcoming of LDA approaches, which overbind atoms by 1%–2% [25]. Inclusion of zero-point and finite temperature atomic motion [26] into LDA results gives an increase of only about 0.2% to the zero temperature lattice constants. Since the values of lattice constants affect vibrational properties, it is important to correct for this limitation of LDA calculations. Here we give results using harmonic and anharmonic IFCs calculated for the following two choices: set 1  $a = 3.138 \text{ \AA}$ ,  $c = 5.109 \text{ \AA}$ , and  $u = 0.377$  determined by energy minimization with a 0.2% increase, and set 2  $a = 3.164 \text{ \AA}$ ,  $c = 5.150 \text{ \AA}$ , and  $u = 0.377$  determined by energy minimization with an increase of 1.0% in the lattice constants, more consistent with measured values. Figure 1 shows the calculated phonon dispersions for wurtzite GaN using set 1 (dashed lines) and set 2 (solid lines) compared with experimental inelastic x-ray data (circles) in the high-symmetry directions [27]. For the low-frequency acoustic branches there is little difference between the two sets. However, the high-lying optic phonon branches are shifted to lower frequencies with the larger lattice constants. These shifts are consistent with the *ab initio* calculations in Ref. [27], which scaled the LDA phonon dispersion by 0.97 to fit the experimental data better.

To determine the anharmonic IFCs, we used a real-space approach similar to that of Ref. [28]. Pairs of atoms were systematically perturbed from the ground state configuration of a large supercell. The resulting Hellman-Feynman forces on all the atoms were calculated via  $\Gamma$ -point self-consistent calculations for a number of different perturbations to obtain numerical derivatives of the forces, which gave the anharmonic IFCs for three-phonon scattering. For wurtzite GaN we used 108 atom supercells and calculated anharmonic IFCs involving a unit cell atom and its 27 nearest neighbors (4th neighbor shell). We also considered the less common metastable zinc blende phase of GaN for

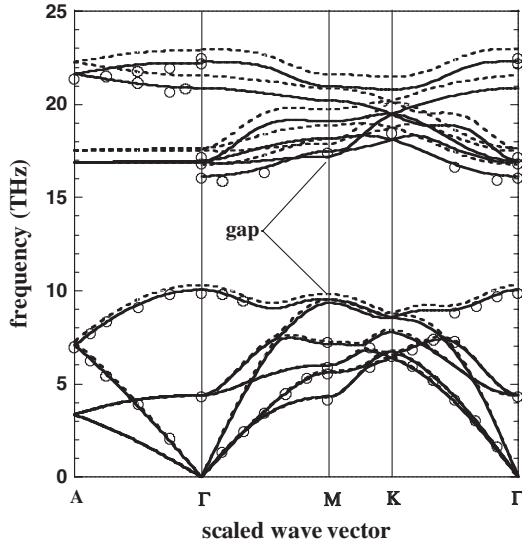


FIG. 1. Calculated phonon dispersion for wurtzite GaN in high-symmetry directions with set 1 (dashed lines) and set 2 (solid lines) lattice constants described in the text. The hollow circles correspond to experimental data determined by inelastic x-ray scattering [27].

which we used 216 atom supercells and calculated anharmonic IFCs for a unit cell atom and its 29 nearest neighbors (3rd neighbor shell). In principle, anharmonic terms from all atomic interactions can enter the scattering matrix elements [Eq. (2)], and longer-range terms may be important in polar semiconductors with Coulomb interactions. To test the effect of including only the nearest neighbors described above, we calculated  $\kappa_L$  for Si, Ge, GaAs, and GaP by using anharmonic IFCs obtained from two approaches: (i) the real-space approach described above and (ii) a reciprocal-space density functional perturbation theory approach [19,20,29] which included short-ranged interactions out to seventh nearest neighbors and long-range Coulomb interactions. We find less than 3% difference in the corresponding room temperature  $\kappa_L$  values from the two approaches.

**Results.**—Figure 2 shows  $\kappa_L(T)$  of wurtzite GaN between 100 and 500 K. The circles and triangles correspond to the measured  $\kappa_L$  of Refs. [6,7], respectively. All curves were determined by using the set 2 lattice constants, which gave the best fit to the experimental data in Fig. 1. The black curves are the calculated  $\kappa_L$  for isotopically pure GaN,  $\kappa_{\text{pure}}$ , in which all Ga atoms are  $^{69}\text{Ga}$ . The red curves are the calculated  $\kappa_L$  for naturally occurring Ga isotope concentrations,  $\kappa_{\text{natural}}$ . The solid curves correspond to  $\kappa_{\text{in}}$  (in-plane transport), and the dashed curves correspond to  $\kappa_{\text{out}}$  (transport along the  $c$  axis).

The phonon-phonon scattering rates increase with temperature, while the phonon-isotope scattering rates are temperature independent [see Eq. (3)]. Thus starting from 500 K, with decreasing  $T$ , phonon-phonon scattering becomes weaker, causing  $\kappa_L$  to rise and making isotope

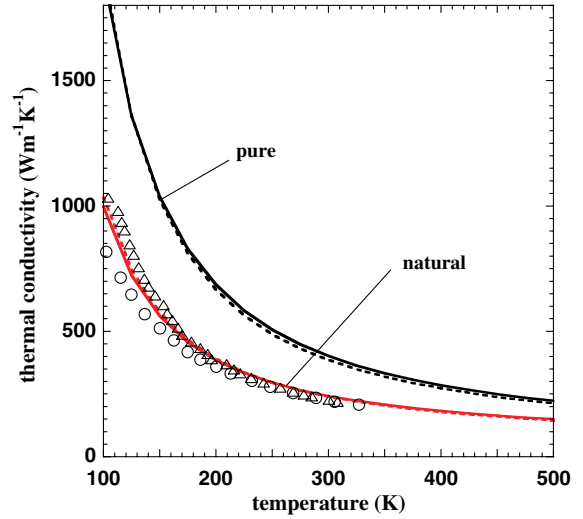


FIG. 2 (color online). Calculated thermal conductivity vs temperature for naturally occurring ( $\kappa_{\text{natural}}$ , two lower red lines) and isotopically pure ( $\kappa_{\text{pure}}$ , two upper black lines) wurtzite GaN given by set 2 lattice constants (described in the text). Solid lines correspond to  $\kappa_{\text{in}}$  and dashed lines to  $\kappa_{\text{out}}$ . The symbols correspond to experimental data from Ref. [6] (circles) and Ref. [7] (triangles).

impurity scattering more important. This is evident from the increasing percent isotope effect  $P$  and seen in the separation between the black and red curves.

The calculated curves for  $\kappa_{\text{natural}}$  are in good agreement with the experimental data [6,7] and have room temperature values  $\kappa_{\text{in}} = 242 \text{ W m}^{-1} \text{ K}^{-1}$  and  $\kappa_{\text{out}} = 239 \text{ W m}^{-1} \text{ K}^{-1}$ . We have estimated the effects of other point defect scattering such as from N isotopic impurities, Ga vacancies, and oxygen (O) substitutions, representing them by the simple mass-difference scattering rates from Eq. (3) and taking the concentrations reported in Ref. [7] (Ga vacancies  $\sim 10^{18}/\text{cm}^3$  and O impurities  $\sim 10^{20}/\text{cm}^3$ ). We find that including N isotopic impurities and O substitutions has almost no effect on  $\kappa_{\text{natural}}$  at room temperature, and including Ga vacancies lowers  $\kappa_{\text{natural}}$  around 2.5%.

The calculated curves for  $\kappa_{\text{pure}}$  are well above the measured data and represent the intrinsic upper limit for  $\kappa_L$  in GaN. At room temperature,  $\kappa_{\text{in}} = 401 \text{ W m}^{-1} \text{ K}^{-1}$  and  $\kappa_{\text{out}} = 385 \text{ W m}^{-1} \text{ K}^{-1}$  corresponding to  $P \sim 60\%–65\%$  for wurtzite GaN. With decreasing temperature, this isotope effect increases, nearing 100% at  $T = 100 \text{ K}$ . At even lower  $T$ , sample size begins to play a role, and the interplay between phonon-phonon and phonon-isotope scattering with that from sample boundaries causes a peak in  $\kappa_L$  (not shown). We have included phonon boundary scattering here by using an empirical relaxation time [9]  $\tau_{\lambda}^B = L/|\vec{v}_{\lambda}|$ , with  $L = 1 \text{ mm}$  as a measure of the sample size consistent with experiment. For all cases,  $\kappa_L$  peaks around  $T = 30 \text{ K}$  with  $\kappa_{\text{pure}} = 22\,000 \text{ W m}^{-1} \text{ K}^{-1}$  being almost 7 times larger than  $\kappa_{\text{natural}} = 3300 \text{ W m}^{-1} \text{ K}^{-1}$  ( $P \sim 600\%$ ).

TABLE I. Calculated mass mismatch, frequency gap between acoustic and highest optic phonon branches, LA phonon frequency at the  $X$  ( $M$ ) point for zinc blende (wurtzite) structure,  $\kappa_{\text{natural}}$  at  $T = 300$  K, and percent isotope effect ( $P$ ) for Ga-based semiconductors.

	$ 1 - \frac{\bar{m}_{\text{Ga}}}{\bar{m}_{\text{anion}}} $	Frequency gap (THz)	$\omega_{\text{LA}}$ (THz)	$\kappa_{\text{natural}}$ ( $\text{W m}^{-1}\text{K}^{-1}$ )	$P$
GaAs	0.07	0	6.70	52	4
GaSb	0.43	0.75	4.83	42	8
GaP	1.25	2.48	7.70	123	14
Cubic GaN	3.98	6.01	10.6	215	68
Wurtzite GaN	3.98	6.11	9.34	242	66

To understand the above findings better, we have calculated the  $\kappa_L$  for zinc blende GaX compounds with  $X = \text{N, P, As, and Sb}$  spanning a wide range of properties, given in Table I. The mass variance parameter for antimony (57.21%  $^{121}\text{Sb}$  and 42.79%  $^{123}\text{Sb}$ ) is  $g_{\text{Sb}} = 6.59 \times 10^{-5}$ , while the negligible isotope mixtures for phosphorus ( $P$ ) and arsenic ( $As$ ) give  $g_P = g_{\text{As}} = 0$ . Figure 3 shows  $P$  vs  $T$  for wurtzite GaN and zinc blende GaN, GaAs, GaSb, and GaP. The smallest  $P$  values occur for GaAs, with  $P = 4.4\%$  at  $T = 300$  K. Our calculated  $\kappa_{\text{natural}}$  and  $P$  for GaAs are in good agreement with  $\kappa_L$  measurements made for isotopically enriched GaAs crystals (99.4%  $^{71}\text{Ga}$  and 0.6%  $^{69}\text{Ga}$ ) which found a  $P = 5\%$  at 300 K [30]. The  $P$  for the GaN polymorphs lie well above those for the other zinc blende compounds.

One might naively assume that GaSb would have the largest enhancement to  $\kappa_L$  with isotopic enrichment because of the larger isotope mixture. However, for a given isotope mixture, it is the interplay between the phonon-phonon scattering and the phonon-isotope scattering that determines  $P$ . Comparing successively GaAs, GaSb, GaP, and GaN (Table I), we find that the phonon-phonon scat-

tering is weakened by (a) increasing mass difference between Ga and anion atoms, which produces a larger acoustic-optic frequency gap, as seen in Fig. 1 for GaN, and (b) increasing atomic bond stiffness and decreasing mass of constituent atoms, which raise the entire phonon spectrum to higher frequencies. Consider point (b) first. Higher overall phonon frequencies reduce the phonon populations of all modes and also reduce the phase space for three-phonon scattering [31], thereby decreasing the phonon-phonon scattering rates. We note that increasing bond stiffness also increases the anharmonic IFCs, thereby enhancing the phonon-phonon scattering matrix elements [Eq. (2)], but the stronger influence from the higher phonon frequencies ultimately leads to reduced scattering rates with increasing bond stiffness in materials such as GaN. We further verified the importance of the frequency scale in determining  $\kappa_L$  and  $P$  by scaling down the full frequency spectrum in wurtzite GaN. The resulting increased phonon-phonon scattering rates significantly lowered  $\kappa_L$  and  $P$ . Reduced acoustic phonon velocities also lowered  $\kappa_L$ .

Consider now point (a). Optic phonons play a critical role in determining  $\kappa_L$  of GaN. Although optic phonons do not significantly contribute directly to a thermal current, they do provide important scattering channels for the heat-carrying acoustic phonons as has been pointed out recently for silicon [19], diamond [20], and lead telluride [32–34]. The extremely large frequency gap in GaN has a dramatic effect on  $\kappa_L$  and  $P$ , because it strongly restricts three-phonon scattering between acoustic and optic phonons [31] through the energy conservation seen in Eq. (2) [35,36]. On the other hand, the isotopic impurity scattering is not much affected by the gap. This point is highlighted by comparison of GaN with silicon. Si has a lighter unit cell mass, higher acoustic phonon frequency scale and acoustic velocities, smaller anharmonic IFCs, and similar isotope scattering (for naturally occurring Si) compared to GaN. These features suggest that Si should have larger  $\kappa_L$  and  $P$  compared to GaN. However, Si has no acoustic-optic frequency gap. Thus, we find that the calculated  $\kappa_{\text{pure}}$  for Si at room temperature ( $155 \text{ W m}^{-1}\text{K}^{-1}$ ) is nearly 3 times smaller than  $\kappa_{\text{pure}}$  for GaN and the calculated  $P$  (7.6%) for Si is almost 9 times smaller than that for GaN [37,38]. These differences stem primarily from the large frequency gap in GaN and the much weaker acoustic-optic phonon scattering that results.

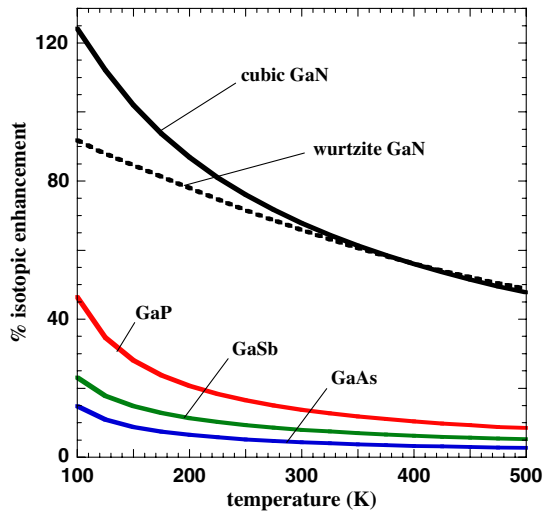


FIG. 3 (color online). Calculated percent isotope effect,  $P$ , vs temperature for GaAs [blue (lowest) line], GaSb [green (lower) line], GaP [red (middle) line], wurtzite GaN (dashed black line), and zinc blende GaN [solid black (highest) line].

**Summary and conclusions.**—We have examined the lattice thermal conductivity  $\kappa_L$  of GaN and its dependence on isotopes by using a microscopic, first principles approach. The calculated  $\kappa_L$  with naturally occurring isotope concentration is in good agreement with measured values over a broad temperature range, and the increase in  $\kappa_L$  with isotopic enrichment ( $\sim 65\%$  at room temperature) is comparable to that of the highest observed enhancements in diamond, graphene, and boron nitride nanotubes. We find that the large  $\kappa_L$  and isotope effect in GaN result from the large Ga isotope mixture, the mass difference between constituent atoms, the light N mass, and strong bond stiffness. The resulting large frequency gap between the acoustic and optic phonon branches and the high phonon frequency scale lead to unusually weak anharmonic phonon-phonon scattering. This interpretation is validated by comparison with GaAs, GaSb, and GaP. The rigorous understanding of phonon-phonon scattering and  $\kappa_L$  presented here for GaN gives important insights into the origin of thermal conductivity and the role of isotopes in other systems.

This work was supported in part by ONR and DARPA (L. L. and T. L. R.). L. L. acknowledges support from the NRC/NRL Research Associateship Program. D. A. B. acknowledges support from the National Science Foundation under Grant No. 1066634 and from the S3TEC, an Energy Frontier Research Center funded by the U.S. Department of Energy, Office of Science, Office of Basic Energy Sciences under Award No. DE-FG02-09ER46577.

- 
- [1] S. N. Mohammad, A. A. Salvador, and H. Morkoç, *Proc. IEEE* **83**, 1306 (1995).
  - [2] K. Chung, C.-H. Lee, and G.-C. Yi, *Science* **330**, 655 (2010).
  - [3] K. Shenai, K. Shah, and H. Xing, in *Proceedings of the IEEE NAECON Conference* (IEEE, New York, 2010), p. 317.
  - [4] S. Dargahi, P. Valizadeh, and S. S. Williamson, in *Proceedings of the Vehicle Power and Propulsion Conference* (IEEE, New York, 2011), p. 1.
  - [5] M. A. Briere, *Power Electron. Eur.* **7**, 29 (2008).
  - [6] G. A. Slack, L. J. Schowalter, D. Morelli, and J. A. Freitas, *J. Cryst. Growth* **246**, 287 (2002).
  - [7] A. Jeżowski, P. Stachowiak, T. Plackowski, T. Suski, S. Krukowski, M. Boćkowski, I. Grzegory, B. Danilchenko, and T. Paszkiewicz, *Phys. Status Solidi B* **240**, 447 (2003).
  - [8] C. Mion, J. F. Muth, E. A. Preble, and D. Hanser, *Appl. Phys. Lett.* **89**, 092123 (2006).
  - [9] J. M. Ziman, *Electrons and Phonons* (Oxford University, London, 1960).
  - [10] A. AlShaikhi, S. Barman, and G. P. Srivastava, *Phys. Rev. B* **81**, 195320 (2010).
  - [11] X.-G. Yu and X.-G. Liang, *Diam. Relat. Mater.* **16**, 1711 (2007).
  - [12] D. T. Morelli, J. P. Heremans, and G. A. Slack, *Phys. Rev. B* **66**, 195304 (2002).
  - [13] A. Witek, *Diam. Relat. Mater.* **7**, 962 (1998).
  - [14] R. Berman, *Diam. Relat. Mater.* **8**, 2016 (1999).
  - [15] X. W. Zhou, S. Aubry, R. E. Jones, A. Greenstein, and P. K. Schelling, *Phys. Rev. B* **79**, 115201 (2009).
  - [16] T. R. Anthony, W. F. Banholzer, J. F. Fleischer, L. Wei, P. K. Kuo, R. L. Thomas, and R. W. Pryor, *Phys. Rev. B* **42**, 1104 (1990).
  - [17] S. Chen, Q. Wu, C. Mishra, J. Kang, H. Zhang, K. Cho, W. Cai, A. A. Balandin, and R. S. Ruoff, *Nature Mater.* **11**, 203 (2012).
  - [18] C. W. Chang, A. M. Fennimore, A. Afanasiev, D. Okawa, T. Ikuno, H. Garcia, Deyu Li, A. Majumdar, and A. Zettl, *Phys. Rev. Lett.* **97**, 085901 (2006).
  - [19] D. A. Broido, M. Malorny, G. Birner, N. Mingo, and D. A. Stewart, *Appl. Phys. Lett.* **91**, 231922 (2007).
  - [20] A. Ward, D. A. Broido, D. A. Stewart and G. Deinzer, *Phys. Rev. B* **80**, 125203 (2009).
  - [21] M. Omini and A. Sparavigna, *Phys. Rev. B* **53**, 9064 (1996).
  - [22] S. I. Tamura, *Phys. Rev. B* **30**, 849 (1984).
  - [23] S. Baroni *et al.*, <http://www.quantum-espresso.org>.
  - [24] H. Schulz and K. H. Thiemann, *Solid State Commun.* **23**, 815 (1977).
  - [25] P. Haas, F. Tran, and P. Blaha, *Phys. Rev. B* **79**, 085104 (2009).
  - [26] P. B. Allen, *Philos. Mag. B* **70**, 527 (1994).
  - [27] T. Ruf, J. Serrano, M. Cardona, P. Pavone, M. Pabst, M. Krisch, M. D'Astuto, T. Suski, I. Grzegory, and M. Leszczynski, *Phys. Rev. Lett.* **86**, 906 (2001).
  - [28] K. Esfarjani and H. T. Stokes, *Phys. Rev. B* **77**, 144112 (2008).
  - [29] G. Deinzer, G. Birner, and D. Strauch, *Phys. Rev. B* **67**, 144304 (2003).
  - [30] A. V. Inyushkin, A. N. Taldenkov, A. Yu Yakubovsky, A. V. Markov, L. Moreno-Garsia and B. N. Sharonov, *Semicond. Sci. Technol.* **18**, 685 (2003).
  - [31] L. Lindsay and D. A. Broido, *J. Phys. Condens. Matter* **20**, 165209 (2008).
  - [32] J. An, A. Subedi, and D. J. Singh, *Solid State Commun.* **148**, 417 (2008).
  - [33] O. Delaire, J. Ma, K. Marty, A. F. May, M. A. McGuire, M.-H. Du, D. J. Singh, A. Podlesnyak, G. Ehlers, M. D. Lumsden, and B. C. Sales, *Nature Mater.* **10**, 614 (2011).
  - [34] Z. Tian, J. Garg, K. Esfarjani, T. Shiga, J. Shiomi, and G. Chen, *Phys. Rev. B* **85**, 184303 (2012).
  - [35] We note that wurtzite GaN has three midfrequency optic phonon branches, which play a role in determining  $\kappa_L$ . The two lower optic branches are quite dispersive and contribute significantly to  $\kappa_L$ . Artificial removal of the highest midfrequency optic branch further reduces the acoustic-optic phonon scattering and enhances  $\kappa_L$ .
  - [36] This point is further supported by the 10% higher calculated room temperature  $\kappa_{\text{natural}}$  and  $\kappa_{\text{pure}}$  obtained by using the set 1 lattice constants for GaN, which give higher optic mode frequencies. Note that the isotope effect predicted by set 1 and set 2 lattice constants is almost the same.
  - [37] Both calculated values for Si are in good agreement the measured values in Ref. [38].
  - [38] A. V. Inyushkin, A. N. Taldenkov, A. M. Gibin, A. V. Gusev and H.-J. Pohl, *Phys. Status Solidi C* **1**, 2995 (2004).